obtaining the conductance of **17** and **18**, we used $NaClO_4$ (3.4×10^{-3} M) with a molar conductance of 194 mho cm^2/mol in acetone for conductivity calculations. ^{15}N NMR data were recorded on an IBM (Bruker) NR/300 FT NMR spectrometer. Electron spin resonance measurements were carried out with a Varian E3 spectrometer equipped with 100-kHz modulation frequency in the X-band region. Microwave power, field, and receiver gain were set at 16, 20 mw 3050, 3200 G, and 3.2×10^2, 6.2×10^3, respectively, for powder spectra of compound **17** at -106 and +20 °C, while in solution (0.075 g/cm^3) at 20 °C these values were set at 50 mw, 3200 G, and 6.2×10^4. The values of time scan, time constant, and modulation amplitude were fixed at 4 m, 1 s, and 10 G, respectively. Gases and volatile liquids were handled in a Pyrex vacuum apparatus equipped with a Heise-Bourdon tube gauge. Elemental analyses were performed by Beller Mikroanalytisches Laboratorium, Göttingen, FRG.

Synthesis of 5-((Difluoroamino)difluoromethyl)tetrazole (7). Diethyl ether (5 mL) and HCl (2.0 mmol) were condensed into a 50-mL Pyrex bulb that contained sodium 5-((difluoroamino)difluoromethyl)tetrazolate (1.5 mmol) at -196 °C. The reactants were warmed slowly to 25 °C, and the mixture was agitated for 2 h. Sodium chloride was removed by filtration. Ether was evaporated, and a quantitative yield of **7** was obtained. Spectral data obtained for **7**: IR (KBr thin film) 3090 b, 2924 b, 2872 w, 2818 b, 1520 m, 1396 s, 1380 m, 1236 vs, 1210 vs, 1191 vs, 1115 s, 1054 s, 1021 s, 990 s, 950 vs, 927 vs, 794 m, 664 m, 633 s, 570 vw, 550 vw, 540 vw, 500 vw cm^{-1}; ^{19}F NMR ϕ 21.55 (NF_2), -100.5 (CF_2); ^1H NMR δ 9.9; ^{15}N NMR ($CDCl_3$/THF) δ -39.73, -65.21. Anal. Calcd for $C_2HF_4N_5$: C, 14.03; H, 0.59; N, 40.93. Found: C, 13.87; H, 0.62; N, 40.93.

Synthesis of 8-13. A small excess of NOCl or CNCl (2.2 mmol) was added to compound **4**, **5**, or **6** (1.5 mmol) in THF (5 mL) in a 50-mL Pyrex bulb at -196 °C. The reactants were warmed slowly to 25 °C, and the mixture was agitated for 24-36 h. The mixture was filtered to remove NaCl. Solvent and excess NOCl and CNCl were evaporated to give ~90% yields of compound **8-13**. Spectral data obtained for **8** (A-B): IR (KBr pellet) 1703 s (NO), 1672 s (NO), 1560 s, 1516 s, 1498 m, 1462 m, 1447 m, 1417 m, 1336 m, 1316 s, 1236 vs, br, 1202 vs, br, 1113 s, 1140 vs, 1023 vs, 979 vs, 951 vs, 925 vs, 885 vw, 796 m, 762 w, 670 m, 635 m cm^{-1}; ^{19}F NMR ϕ 20.58, 20.07 (NF_2), -100.3, -100.6 (CF_2). Spectral data obtained for **9** (A-B): IR (KBr pellet) 1687 m (NO), 1655 m, 1562 vw, 1523 vw, 1490 m, 1469 vw, 1420 m, 1342 vs, 1213 vs, 1160 vs, 1087 s, 1041 m, 976 vs, 826 vw, 751 vs, 735 w, 638 m, 545 w cm^{-1}; ^{19}F NMR ϕ -84.56 (A-B two triplets, J = 2.56 Hz), -115.02 (multiplet, two overlapping quartets). Spectral data obtained for **10** (A-B): IR (KBr pellet) 2900 vw (THF), 1720 s (NO), 1520 s, 1500 w, 1450 m, 1440 m, 1410 w, 1310 m, 1270 vs, 1220 vs, 1050 vs, 1010 vs, 940 m, 770 m, 755 s, 730 m, 680 s, 520 w cm^{-1}; ^{19}F NMR ϕ -63.48, -63.71 (CF_3). Spectral data obtained for **11** (A-B): IR (KBr pellet) 2185 s (CN), 1580 s, 1525 s, 1435 s, 1400 w, 1380 w, 1345 w, 1210 vs, br, 1050 s, 980 s, 965 w, 930 s, 845 w, 820 w, 770 w, 675 vw, 640 w, 550 w cm^{-1}; ^{19}F NMR ϕ 20.0 (NF_2), -100.0 (CF_2). Spectral data obtained for **12** (A-B): IR (KBr pellet) 2263 vw, 2245 vw, 2236 vw, 2180 s (CN), 2156 s (CN), 1586 vs, 1530 vs, 1460 s, 1395 s, 1337 s, 1221 vs, 1195 vs, 1183 vs, 1160 vs, 1075 m, 1031 m, 986 s, 970 s, 925 w, 831 m, 817 m, 751 w, 740 w, 710 w cm^{-1}; ^{19}F NMR ϕ -84.10, -84.98 (CF_3), -114.68, -115.3 (CF_2). Spectral data obtained for **13** (A-B): IR (KBr pellet) 2207 m, 2146 s (CN), 1667 vs, 1638 vs, 1573 s, 1553 vs, 1421 m, 1403 m, 1383 vs, 1209 vs, 1085 vw, 1041 s, 988 m, 830 m, 750 m, 730 w, 710 w cm^{-1}; ^{19}F NMR ϕ -64.38, -64.61 (CF_3).

Synthesis of 14-16. A solution of $(CNCl)_3$ (1.6 mmol) in THF (5 mL) was added slowly under anhydrous conditions to a solution of **4**, **5**, or **6** (1.5 mmol) in THF (5 mL). The mixture was agitated for 36 h in the dark. NaCl was removed by filtration. Partial removal of THF and recrystallization from a 50:50 chloroform-petroleum ether mixture at 0 °C gave ~60% yields of pure **14-16**. Spectral data obtained for **14** (A-B): IR (KBr disk) 1604 vs, 1581 vs, 1537 m, 1428 vs, 1387 vs, 1364 w, 1305 vw, 1187 vs, 1114 w, 1046 vs, 980 vs, 950 s, 925 vs, 839 s, 817 m, 795 w, 670 w, 632 w, 604 w, 540 m, 483 w cm^{-1}; ^{19}F NMR ϕ 22.53, 22.07 (NF_2), -100.25, -100.54 (CF_2). Spectral data obtained for **15** (A-B): IR (KBr disk) 1579 vs, 1476 vw, 1428 vs, 1401 w, 1384 m, 1340 s, 1219 vs, 1181 s, 1156 vs, 1071 m, 1033 vw, 973 vs, 839 m, 828 m, 809 m, 769 w, 751 s, 635 m cm^{-1}; ^{19}F NMR ϕ -83.69, -84.32 (CF_3), -113.92, -113.59 (CF_2). Spectral data obtained for **16** (A-B): IR (KBr disk) 1705 vs, 1509 m, 1461 s, 1419 s, 1399 s, 1208 m, 1170 vs, 1045 m, 985 vw, 850 m, 765 m, 530 s cm^{-1}; ^{19}F NMR ϕ -64.62, -64.33.

Synthesis of 17 and 18. Into a 50-mL Pyrex bulb containing compound **5** or **6** in THF (5 mL) at -196 °C was condensed CNCl (2.2 mmol). A solution of $CuCl_2 \cdot 2H_2O$ (1 mmol) in THF (5 mL) was added to the frozen solution. The reaction mixture was warmed slowly to room temperature and was agitated for 48 h. Solid NaCl and some unidentified insoluble copper complex was removed by filtration. Crystallization and recrystallization from a 50:50 mixture of petroleum ether-THF gave pure compound **17** or **18** in 25-30% yield. The purity was determined by TLC. Spectroscopic data obtained for **17**: IR (KBr disk) 3300-2900 br (THF), 2232 s (CN), 2169 m (CN), 1656 s, 1570 m, 1513 m, 1446 m, 1367 vw, 1345 w, 1330 w, 1179 vs, 1072 m, 1037 s, 774 m, 756 s, 740 m cm^{-1}; ^{19}F NMR (in THF) ϕ -66.67 vbr (3), -77.49 br (1), -82.64 br (1). Anal. Calcd for $Cu_2C_{34}H_{16}F_{30}N_{46}O_2$: C, 22.70; H, 0.89; N, 35.84; Cu, 7.06. Found: C, 23.27; H, 1.11; N, 37.29; Cu, 6.97. Spectral data obtained for **18**: IR (KBr disk) 3300-2900 br (THF), 2161 s (CN), 1600-1500 vbr, 1376 m, 1337 s, 1220 vs, 1162 vs, 1073 w, 1038 w, 992 w, 972 s, 901 w, 882 w, 751 s, 637 w, 540 vw, 484 vw, 409 vw cm^{-1}; ^{19}F NMR (in THF) ϕ -82.01 br, -84.55 br, -115.03 br, -120.75 br. Anal. Calcd for $CuC_{38}H_{16}F_{40}N_{38}O_2$: C, 24.52; H, 0.86; F, 40.9; Cu, 3.42. Found: C, 24.84; H, 0.94; F, 41.5; Cu, 3.54.

Acknowledgment is made to the donors of the Petroleum Research Fund, administered by the American Chemical Society, to the NSF (Grants CHE-8404974 and CHE-8703790), and to the AFOSR (Grant 87-0067).

Contribution from the Department of Chemistry, Texas A&M University, College Station, Texas 77843-3255

Dinuclear Complexes of a [30]$Py_2N_4O_4$ Macrocyclic Ligand Containing Two α,α'-Bis(aminomethyl)pyridine Moieties. Comparison with Analogous 22- and 24-Membered Macrocyclic Ligands

Rached Menif, Dian Chen, and Arthur E. Martell*

Received May 1, 1989

The synthesis of the hexaaza macrocycle L = 3,12,20,29,35,36-hexaaza-6,9,23,26-tetraoxatricyclo[29.3.1.1^{14,18}]hexatriaconta-1(34),14,16,18(36),31(35),32-hexaene (O2-BISBAMP) is reported. Protonation as well as metal binding constants with Cu(II), Co(II), Ni(II), and Zn(II) have been determined at 25.0 °C and 0.100 M ionic strength. Mononuclear and dinuclear chelates of these metal ions are identified in all systems investigated. Mono- and diprotonated and monohydroxy mononuclear complexes of O2-BISBAMP are formed with all metal ions studied. Strong tendencies toward hydroxide ion bridging between the two metal centers in the dinuclear complexes were not found except for the dinuclear Cu(II) complex. The metal ion affinities as well as the binucleating and bridging tendencies of L are compared to those of analogous ligands containing macrocyclic rings.

Introduction

The protonation constants and metal ion stability constants in aqueous solution of the binucleating macrocyclic ligands C-BISBAMP (3,8,16,21,27,28-hexaazatricyclo[21.3.1.1^{10,14}]octacosa-1(26),10(28),11,13,23(27),24-hexaene, **2**) and O-BISBAMP (3,9,17,23,29,30-hexaaza-6,20-dioxatricyclo[23.3.1.1^{11,15}]triaconta-1(28),11,13,15(30),25(29),26-hexaene, **3**) have been measured by Arnaud-Neu et al.[1] and Basalotte et al.,[2] respectively.

(1) Arnaud-Neu, F.; Sanchez, M.; Schwing-Weill, M.-J. *Helv. Chim. Acta* **1985**, *68*, 840.
(2) Basalotte, M. G.; Martell, A. E. *Inorg. Chem.* **1988**, *27*, 4219.

0020-1669/89/1328-4633$01.50/0

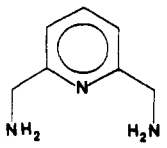

1 2,6-bis(aminomethyl)pyridine, BAMP

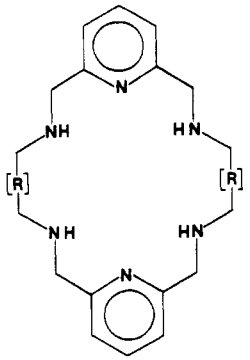

2 R = $(CH_2)_2$, C-BISBAMP

3 R = CH_2OCH_2, O-BISBAMP

4 R = $(CH_2OCH_2)_2$, O2-BISBAMP

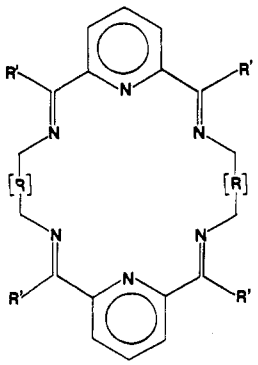

5 R' = CH_3 R = $(CH_2OCH_2)_2$

6 R' = H R = $(CH_2OCH_2)_2$

7 R' = CH_3 R = CH_2

8 R' = H R = $(CH_2)_2$

9 R' = CH_3 R = $(CH_2)_3$

The macrocycles named [22]Py_2N_4[1] and BISBAMP[2] in previous papers are renamed respectively C-BISBAMP (for the macrocycle with four-atom bridges) and O-BISBAMP (for the macrocycle with five-atom ether oxygen bridges). Mononuclear complexes ML^{n+} were identified for M^{n+} = Co^{2+}, Ni^{2+}, Cu^{2+}, and Zn^{2+} with the macrocycle C-BISBAMP, but the dinuclear species M_2L^{2n+} was found only with M^{n+} = Cu^{2+}. No μ-hydroxo dinuclear complexes were detected. In contrast with the behavior of C-BISBAMP, O-BISBAMP was found to form mononuclear as well as binuclear complexes with the four metal ions cited above. The dinuclear complexes showed a strong tendency toward hydroxide ion bridging between the two metal ions. Furthermore, the binuclear cobalt(II) complex yielded in the presence of dioxygen a (μ-hydroxo)(μ-peroxo)cobalt(III) adduct that forms three hydroxo species.

In view of these results, it appeared of interest to determine the possible role of the length and nature of the bridging atoms between the binding units in stabilizing the dinuclear complexes and promoting the binding of bridging hydroxide ions and dioxygen between the two metal centers. One way of testing these ideas is to determine analogous binding constants including hydroxide bridging constants for a macrocyclic ligand having a structure similar to that of C-BISBAMP and O-BISBAMP but with longer bridges.

In this paper, we report the synthesis of the macrocyclic ligand 3,12,20,29,35,36-hexaaza-6,9,23,26-tetraoxatricyclo-[29.3.1.1^{14,18}]hexatriaconta-1(34),14,16,18(36),31(35),32-hexaene (O2-BISBAMP, **4**). The Schiff base analogues of O2-BISBAMP, **5** and **6**, as well as their mononuclear and dinuclear complexes have been extensively studied by Nelson et al.[3] However, these compounds are easily hydrolyzed and are not stable in aqueous solution. A dinuclear copper(I) complex of O2-BISBAMP has also been prepared by Burnett et al.[4] by BH_4^- reduction of the tetrathiocyanate salt of the dinuclear lead(II) complex of **6**, followed by transmetalation to yield $Cu^I_2L(ClO_4)_2$, where L = **4**. The metal-free ligand O2-BISBAMP (**4**) was not reported by these investigators. In the present work, the protonation constants as well as the equilibrium constants for the coordination of the ligand O2-BISBAMP with Cu(II), Ni(II), Co(II), and Zn(II) have been measured. The stabilities of metal complexes of C-BISBAMP, O-BISBAMP, and O2-BISBAMP are compared.

Experimental Section

Materials. 2,6-Pyridinedicarboxaldehyde (98%) and $NaBH_4$ (98%) were used as supplied by Aldrich. 1,8-Diamino-3,6-dioxaoctane was prepared by the method of Bogatskii et al.[5] The Pb(II) complex of the macrocyclic Schiff base was prepared by a modification of the method of Cook et al.[6] Stock solutions of Cu(II), Ni(II), Co(II), and Zn(II) nitrates for potentiometric work were prepared, and their concentrations were determined by titration with EDTA with the appropriate indicators.[7] A carbonate-free 0.1047 M KOH solution was prepared from a Dilut-It ampule and standardized with potassium acid phthalate. Reagent grade potassium nitrate was used as supporting electrolyte for all the experiments.

Preparation of O2-BISBAMP ([30]$Py_2N_2O_4$). To a 1-L three-necked flask with a thermometer, a gas inlet tube, and a reflux condenser was introduced 380 mL of MeOH, and dry argon was passed through the flask to remove the air. The flask was warmed with stirring in an oil bath to 40 °C, and 1.00 g of 2,6-pyridinedicarboxaldehyde, 2.50 g of Pb(SCN)$_2$, and 1.10 g of 1,8-diamino-3,6-dioxaoctane was added. The temperature of the mixture was maintained at 40 °C for 1 h, after which the argon stream was terminated. The reaction mixture was heated to 45 °C; then 2.20 g of $NaBH_4$ was added to the solution. After the addition of the $NaBH_4$ was complete, the reaction solution was stirred an additional 20 min and then cooled. Metallic lead that precipitated was filtered off. The filtrate was evaporated to dryness; 20 mL of 1.00 M aqueous EDTA (pH 9.7) and 100 mL of $CHCl_3$ were added to the flask to extract the free ligand and remove the Pb(II). The $CHCl_3$ solution was twice washed with 20 mL of saturated NaCl solution. The organic phase was filtered and dried with anhydrous Na_2SO_4. The solution was allowed to stand for 2 h and then filtered. The filtrate was evaporated to dryness. A total of 1.78 g of oily material was obtained. The yield of crude macrocycle was 90%. To convert the free base to the HCl salt, the oily material was dissolved in 20 mL of 1:1 ethanol–ether mixed solvent and dry HCl gas was passed into the solution. The hydrochloride salt started to precipitate immediately. When the solution was saturated with HCl gas, the product was filtered and washed with ether. The compound was recrystallized from ethanol and dried for 5 h at 60 °C under vacuum. A total of 1.70 g of product was obtained (overall yield 67%). ^{1}H NMR (free base, in $CDCl_3$): δ 7.8 (t, 2 H, pyridine), 7.3 (d, 4 H, NH–CH_2), 3.9 (s, 8 H, py–CH_2), 3.7 (m, 16 H, O–CH_2, CH_2–O), 2.9 (t, 8 H, NH–CH_2), 2.6 (s, 4 H, NH). ^{1}H NMR (HCl salt, in D_2O): δ 8.1 (t, 2 H, pyridine), 7.7 (d, 4 H, pyridine), 4.7 (s, 8 H, py–CH_2), 4.0 (m, 16 H, –OCH_2, –CH_2), 3.5 (t, 8 H, $NHCH_2$). Anal. Calcd for $C_{26}H_{42}N_6O_4 \cdot 4HCl \cdot 2.5H_2O$ (fw 693.66): C, 45.02; H, 7.41; N, 12.12. Found: C, 45.15; H, 7.33; N, 12.00.

Potentiometric Equilibrium Measurements. Potentiometric equilibrium measurements were carried out in the absence and in the presence of metal ions, with a Corning Model 150 digital pH meter in a water-jacketed reaction vessel maintained at 25.0 °C. The ionic strength of the medium was maintained at 0.100 M by the addition of KNO_3. The potentiometric cell was fitted with glass and calomel electrodes that were calibrated with standard aqueous HCl solution to read –log [H^+] directly. The potentiometric measurements were carried out under an atmosphere of argon. Equilibrium measurements were made in 50-mL solutions containing O2-BISBAMP free of metal ions and on solutions containing 1:1 and 2:1 ratios of metal ions to O2-BISBAMP. The amount of ligand in the 50-mL solutions was 0.100 mmol.

Computations. The equilibrium constants were determined by using the program BEST[8] written in this laboratory. No attempts were made

(3) Nelson, M.; McCann, M.; Stevenson, C.; Drew, M. G. B. *J. Chem. Soc., Dalton Trans.* **1979**, 1477. Nelson, M.; Knox, V. C.; McCann, M.; Drew, M. G. B. *J. Chem. Soc., Dalton Trans.* **1981**, 1669.

(4) Burnett, M. G.; McKee, V.; Nelson, M.; Drew, M. G. B. *J. Chem. Soc., Chem. Commun.* **1980**, 829.

(5) Bogatskii, A. V.; Lukyaneko, N. G.; Kirichenko, T. I. *Org. Khim.* **1980**, *16*, 1301.

(6) Cook, D. H.; Fenton, D. E.; Drew, M. G. B.; Rodgers, A.; McCann, M.; Nelson, S. M. *J. Chem. Soc., Dalton Trans.* **1979**, 414.

(7) Schwarzenbach, G.; Flaschka, H. *Complexometric Titrations*, 2nd English ed.; Methuen: London, 1969.

(8) Motekaitis, R. J.; Martell, A. E. *Determination and Use of Stability Constants*; VCH: New York, 1989.

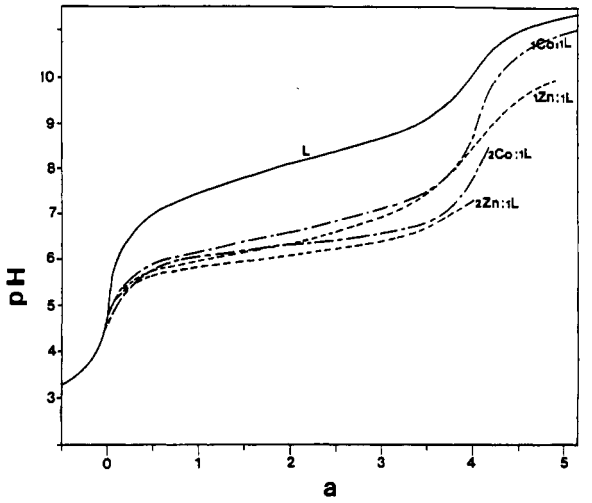

Figure 1. Potentiometric equilibrium curves for O2-BISBAMP and for 1:1 and 2:1 metal–ligand systems with Co(II) and Zn(II) (a = moles of 0.100 M KOH added per mole of ligand; μ = 0.100 M (KNO_3); t = 25 °C).

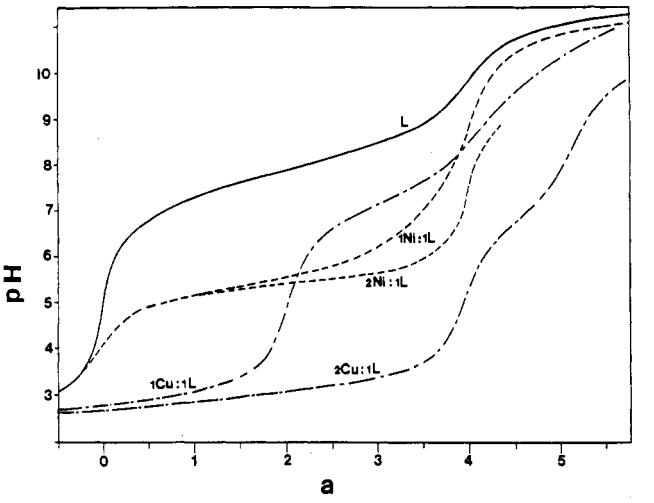

Figure 2. Potentiometric equilibrium curves for O2-BISBAMP and for 1:1 and 2:1 metal–ligand systems with Cu(II) and Ni(II) (a = moles of 0.100 M KOH added per mole of ligand; μ = 0.100 M (KNO_3), t = 25 °C).

Table I. Successive Protonation Constants of O2-BISBAMP, O-BISBAMP, C-BISBAMP, and BAMP

	log K_i^H [a]			
i	O2-BISBAMP[b]	O-BISBAMP[c]	C-BISBAMP[d]	BAMP[e]
1	8.76 (0.03)	8.75	9.11	9.53
2	8.11 (0.02)	7.94	8.32	
3	7.68 (0.01)	7.36	7.12	9.15
4	6.97 (0.01)	6.79	3.72	

[a] $K_i^H = [H_iL^{i+}]/[H][H_{i-1}L^{(i-1)+}]$. [b] This work ($\mu$ = 0.100 M (KNO_3), t = 25 °C). [c] Reference 2 (μ = 0.100 M (KNO_3), t = 25 °C). [d] Reference 1 (μ = 0.0100 M ($NaClO_4$), t = 25 °C). [e] Reference 14 (μ = 1.00 M ($NaNO_3$), t = 20 °C).

to "invent" additional species for the purpose of obtaining a better fit of the experimental data. The species introduced were limited to those that can be justified on the basis of established principles of coordination chemistry. Species distribution curves were generated with the aid of the program SPE[8] written in this laboratory.

Results and Discussion

Protonation Constants of O2-BISBAMP. The potentiometric equilibrium curves of O2-BISBAMP·4HCl (Figure 1) possess two inflections, at a = 0 and a = 4, where a is the number of moles of base added per mole of ligand. The buffer region between p[H] 7 and 9 corresponds to the neutralization of the four aliphatic nitrogens. The curve in the region from a = −2 to a = 0 can be fitted by assuming neutralization of the strong acid H^+ by the strong base OH^-. Therefore, it is found as in the cases of C-BISBAMP and O-BISBAMP that the pyridine nitrogens are not protonated even under strongly acidic solutions as low as p[H] 2. The corresponding protonation constants are lower than 10^2 and could not be measured accurately by potentiometric titration. The logarithmic values of the protonation constants are listed in Table I, along with those of C-BISBAMP and O-BISBAMP. The proton association constants of O-BISBAMP and O2-BISBAMP were found to be very similar. More particularly, the first protonation constants are identical for both macrocycles while the remaining constants of O2-BISBAMP are slightly lower than those of O-BISBAMP. Since Coulombic repulsion effects start to appear after the first protonation is completed, the lower values of K_i^H (i = 2, 3, 4) for O-BISBAMP may be attributed to the shorter ether bridge causing more Coulombic repulsion. It is seen that the first protonation constant of C-BISBAMP is higher than the corresponding constants of the two other macrocycles. Neither Coulombic repulsions nor statistical factors can be the cause of this difference. It is proposed that the lower basicity in the case of O-BISBAMP and O2-BISBAMP is due to the electron-withdrawing ether oxygens in the bridges between the two BAMP moieties. Similar findings have been reported[9] for O-BISTREN versus C-BISTREN.

The protonation constants of O2-BISBAMP and O-BISBAMP are seen to drop steadily by about 0.5–0.7 log unit as the number of protons on the ligand increases. The situation is quite different for C-BISBAMP, where the difference in the successive protonation constants (log K_1^H − log K_2^H = 0.8; log K_2^H − log K_3^H = 1.2; log K_3^H − log K_4^H = 3.4) increases considerably. A plausible explanation for this difference in behavior is a much greater constraint of the BAMP units in C-BISBAMP, which results in Coulombic repulsions between the positively charged protonated amino nitrogens that are much higher than those in the diprotonated BAMP and polyprotonated O-BISBAMP and O2-BISBAMP macrocyclic ions. In the latter, the protonated amino nitrogens are able to assume extended conformations in aqueous solution that lessen the Coulombic repulsions between the positively charged protonated units.

Metal Chelates of O2-BISBAMP. The potentiometric equilibrium curves of 1:1 ratio of metal to ligand (Figures 1 and 2) show a distinctive behavior for Cu(II) relative to that of the three other metal ions. Cu(II) reacts more strongly at considerably lower p[H] values and displaces protons from the tetraprotonated form of the ligand. In the cases where the ratio of metal to ligand is 2:1, slow p[H] drifting was observed after the break of a > 4 for Co(II), Ni(II), and Zn(II) due to metal hydroxide precipitation. All data beyond a = 4 were thus not used for equilibrium constant determinations. The 2:1 Cu(II)–L system behaves differently: the potentiometric curve remains much lower than the corresponding curve of the 1:1 Cu–L system between a = 2 and a = 4, indicating that Cu(II) interacts strongly with the mononuclear complex species. The p[H] readings remain stable for more than 20 min even at high p[H]. The titration curve possesses two breaks at a = 4 and a = 5, which is consistent with the formation of strongly bound hydroxy species. The equilibrium constants that were found necessary to account for the potentiometric equilibrium data of the type illustrated in Figures 1 and 2 are listed in Tables II and III together with the corresponding values of O-BISBAMP, C-BISBAMP, and BAMP. It is seen that the computer analysis of the data reveals the existence of a number of species considerably larger than those that were obvious by visual inspection of the potentiometric equilibrium curves. Mono- and diprotonated species as well as monohydroxy species were found for all metal ions studied in the 1:1 systems. In the 2:1 systems, dinuclear complexes and their hydroxo adducts were detected in all cases. For Cu(II), polyhydroxo dinuclear complexes $Cu_2L(OH)_n$ (n = 1, 2, 3) were needed to fit the data in the basic

(9) Motekaitis, R. J.; Martell, A. E.; Murase, I.; Lehn, J.-M.; Hosseini, M. W. *Inorg. Chem.* **1988**, *27*, 3630.

Table II. Logarithms of the Formation Constants of Cu(II) Complexes of O2-BISBAMP,[a] O-BISBAMP,[b] C-BISBAMP,[c] and BAMP[d]

quotient, Q	O2-BIS-BAMP	O-BIS-BAMP	C-BIS-BAMP	BAMP
$[H_2ML]/[HML][H]$	6.19	5.24	*e*	*e*
$[HML]/[ML][H]$	7.04	7.44	*e*	*e*
$[ML]/[M][L]$	14.81	15.19	12.83	15.70
$[ML(OH)][H]/[ML]$	−10.0	−9.70	*e*	−8.8
$[M_2L]/[ML][M]$	10.95	8.82	5.73	*f*
$[M_2L(OH)][H]/[M_2L]$	−6.5	−6.51	*e*	*e*
$[M_2L(OH)_2][H]/[M_2L(OH)]$	−9.4	−9.12	*e*	*e*
$[M_2L(OH)_3][H]/[M_2L(OH)_2]$	−11.5	*e*	*e*	*e*
$[M_2HL]/[H][M_2L]$	2.94	*e*	*e*	*e*

[a] This work (σ_{fit} = 0.006 (1:1), σ_{fit} = 0.007 (2:1), μ = 0.100 M (KNO_3), t = 25 °C). [b] Reference 2 (μ = 0.100 M (KNO_3), t = 25 °C). [c] Reference 1 (μ = 0.0100 M ($NaClO_4$), t = 25 °C). [d] Reference 14 (μ = 1.00 M ($NaNO_3$), t = 20 °C). [e] Species not found. [f] $[ML_2]/[ML][L] = 10^{+5.4}$.

region. The binuclear Cu(II) system is also unique in the formation of an unusual protonated species, Cu_2HL, in acid solution. This behavior was not observed with the other metal ions investigated.

Cobalt Dioxygen Complex. When the 2Co:L potentiometric titration is carried out in the presence of dioxygen, a strong brown color starts developing at a = 4, indicating the formation of a dioxygen adduct of the cobalt complex species.[10] However, continuous drifting of the p[H] readings once the brown color has appeared render it not possible to determine K_{O_2} by potentiometric titration. The binding of O_2 to the cobalt(II) complex species present in solution was found to be irreversible since a red color (probably indicative of the oxidation of Co(II) to Co(III)) was detected upon acidification of the brown solution. The very light pinkish color that existed at the beginning of the titration at low p[H] before the formation of the dioxygen complex was not recovered. It is suspected that the dioxygen adduct, once formed, is not stable but is a reactive species that undergoes degradation reactions responsible for the continuous drifting of the p[H] reading. The absorbance of the LMCT band ($\pi^*(O_2) \rightarrow d_{z^2}$) at 370 nm of a freshly prepared dioxygen adduct solution was followed by UV–vis spectroscopy and was found to decrease at room temperature under anaerobic conditions (Figure 6). After 4 days, well beyond the span of the degradation reaction, the reaction mixture was exposed to dioxygen and a small increase in the absorbance of the LMCT band at 370 nm indicated additional O_2 uptake by the solution (Figure 6). The cobalt ions were removed[11] from the solution as CoS, and the aqueous solution was concentrated under reduced pressure to recover the organic material. The extraction was only partially successful (yield 40–45%), and the recovered ligand was found to display the same ^1H NMR spectrum as O2-BISBAMP and was concluded to be the original unchanged ligand. Oxidative dehydrogenation was proposed by Burnett et al.[4] as the degradation reaction occurring upon oxygenation of Cu^I_2(O2-BISBAMP) in MeCN. The reaction mixture described above was thus tested for the presence of the aldehyde function by standard methods.[11] Indeed, oxidative dehydrogenation of the ligand would lead to the formation of imine bonds, which would yield the pyridine-2-carboxaldehyde moiety in acidic aqueous solution.[12] No detectable amount of aldehyde was found, but one cannot rule out the possibility that 10–15% of the ligand O2-BISBAMP is dehydrogenated. A sampled dc polarogram[13] of the dioxygen adduct solution in the p[H] range 7.0–9.0 revealed the presence of both Co(II) and Co(III), indicating the presence in solution of both the Co(II) complex and its dioxygen adduct.

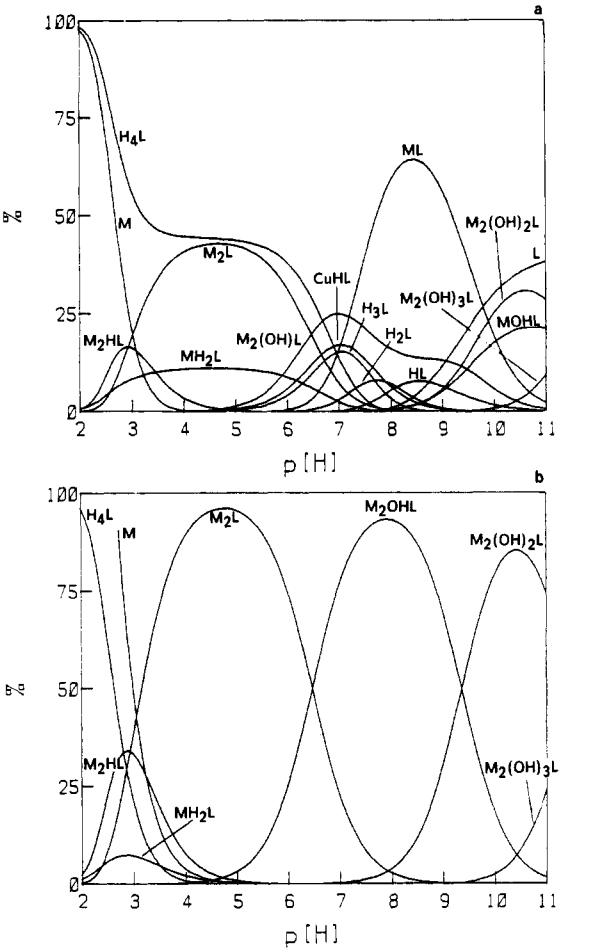

Figure 3. (a) Species distribution diagram of the 1:1 Cu(II)–O2-BISBAMP system as a function of −log $[H^+]$ ($T_L = T_{Cu} = 2.00 \times 10^{-3}$ M). (b) Species distribution diagram of the 2:1 Cu(II)–O2-BISBAMP system as a function of −log $[H^+]$ ($T_L = {}^1/_2 T_{Cu} = 2.00 \times 10^{-3}$ M).

The polarogram of the oxidation product solution revealed the presence of a slightly larger amount of Co(III) and a slightly smaller amount of Co(II). It was not possible, however, to assess quantitatively the extent of oxidation of the metal because of the variety of species present in the solution before the degradation reaction took place. It is suggested that several pathways[14] are possible for the oxidative degradation: oxidation of Co(II) to Co(III), dehydrogenation of the ligand, and possibly other nonidentified reactions involving the ligand.

Species Distribution Curves. On the basis of the equilibrium data in Tables I–III, the distributions of individual metal complex species were calculated as a function of p[H] for 1:1 and 2:1 molar ratios of M to L with M = Co(II), Ni(II), Cu(II), and Zn(II) (Figures 3–5). Zn(II) was omitted due to the close similarities of its metal binding constants with those of Co(II). According to the model at p[H] = 5–8 the dinuclear complexes Co_2L and Ni_2L exist in solution and are the predominant species at p[H] higher than 7 but prior to precipitation (Figures 4b and 5b). It is interesting to note that $Co_2L(OH)$ and $Ni_2L(OH)$ never exceed 25% with respect to the total analytical concentration of the ligand. In the case of Cu(II), it is seen that considerable concentrations of Cu_2L and $Cu_2(OH)L$ form in the 1:1 system, CuL being the predominant species only in the narrow p[H] range 7.5–9.5 (Figure 3a). The system containing a 2:1 molar ratio of Cu(II) to ligand has very simple species distribution curves: Cu_2L is the principal species above p[H] = 4 and is converted around p[H] = 6 to $Cu_2L(OH)_n$ as the p[H] increases (n = 1, 2, 3; Figure 3b).

Comparison of Stabilities of Complexes of BAMP, C-BISBAMP, O-BISBAMP, and O2-BISBAMP. The stability constant

(10) Niederhoffer, E. C.; Timmons, J. H.; Martell, A. E. *Chem. Rev.* **1984**, *84*, 137.
(11) Raleigh, C. J. Ph.D. Dissertation, Texas A&M University, 1984.
(12) Basak, A. K.; Martell, A. E. *Inorg. Chem.* **1988**, *27*, 1948.
(13) Harris, W. R.; McLendon, G.; Martell, A. E.; Bess, R. C.; Mason, M. *Inorg. Chem.* **1980**, *19*, 21.
(14) Martell, A. E.; Basak, A. K.; Raleigh, C. J. *Pure Appl. Chem.* **1988**, *60*(8), 1325.

Table III. Logarithms of the Formation Constants of Co(II), Ni(II), and Zn(II) Complexes of O2-BISBAMP,[a] O-BISBAMP,[b] and C-BISBAMP[c]

	$[H_2ML]/[HML][H]$	$[HML]/[ML][H]$	$[ML]/[M][L]$	$[ML(OH)][H]/[ML]$	$[M_2L]/[ML][M]$	$[M_2L(OH)][H]/[M_2L]$
			M = Co(II)			
O2-BISBAMP[d]	6.43	6.89	8.86	−11.2	4.1	−8.4
O-BISBAMP	*g*	7.12	9.05	−9.97	3.00	−7.9
C-BISBAMP	*g*	*g*	7.36	−8.10	*g*	*g*
			M = Ni(II)			
O2-BISBAMP[e]	6.29	7.19	11.30	−12.0	5.2	−8.7
O-BISBAMP	4.65	7.40	11.25	−10.23	3.73	−5.11
C-BISBAMP	*g*	*g*	9.40	−12.78	*g*	*g*
			M = Zn(II)			
O2-BISBAMP[f]	6.42	7.08	8.70	−9.70	3.9	−6.8
O-BISBAMP	*g*	7.45	8.89	−9.52	3.80	−7.07
C-BISBAMP	*g*	*g*	6.92	−7.33	*g*	*g*

[a] This work (μ = 0.100 M (KNO_3), t = 25 °C). [b] Reference 2 (μ = 0.100 M (KNO_3), t = 25 °C). [c] Reference 1 (μ = 0.0100 M ($NaClO_4$), t = 25 °C). [d] σ_{fit} = 0.011 (1:1), 0.007 (2:1). [e] σ_{fit} = 0.028 (1:1), 0.027 (2:1). [f] σ_{fit} = 0.011 (1:1), 0.013 (2:1). [g] Species not found.

Table IV. Logarithms of the Successive Binding Constants[a] of M(II) to H_2L, HL, and L (M(II) = Cu(II), Ni(II), Co(II), Zn(II); L = O2-BISBAMP).

	M(II)			
quotient, Q	Cu(II)	Ni(II)	Co(II)	Zn(II)
$[MH_2L]/[M][H_2L]$	11.7	7.91	5.31	5.29
$[MHL]/[M][HL]$	13.09	9.73	6.99	6.98
$[ML]/[M][L]$	14.81	11.30	8.86	8.70

[a] These constants are calculated from the data in Tables II and III.

Table V. Logarithms of the Successive Binding Constants[a] of M(II) to H_2L, HL, and L (M(II) = Cu(II), Ni(II), Co(II), Zn(II); L = O-BISBAMP)

	M(II)			
quotient, Q	Cu(II)	Ni(II)	Co(II)	Zn(II)
$[MH_2L]/[M][H_2L]$	11.18	6.61		
$[MHL]/[M][HL]$	13.88	9.90	7.42	7.59
$[ML]/[M][L]$	15.19	11.25	9.05	8.89

[a] These constants are calculated from the data in Tables II and III.

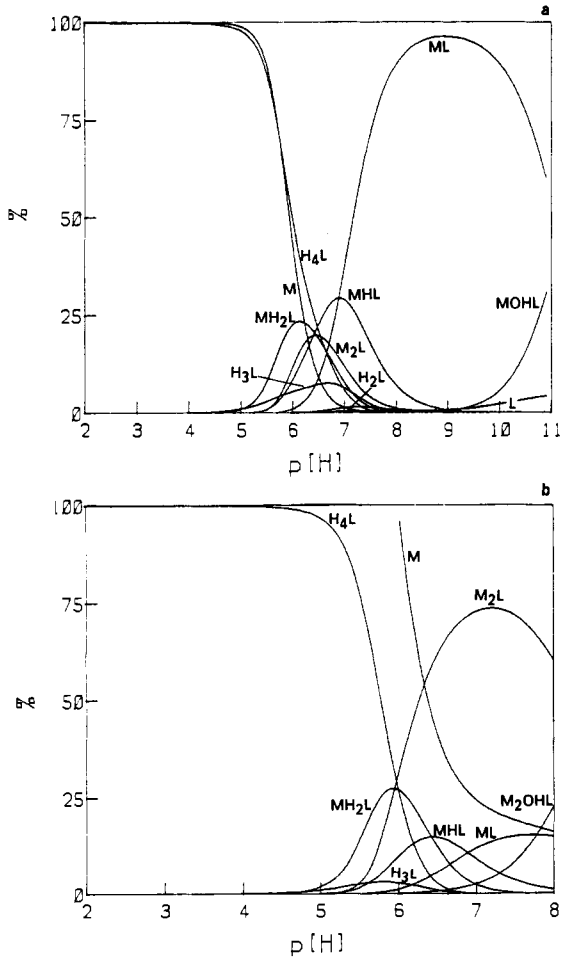

Figure 4. (a) Species distribution diagram of the 1:1 Co(II)–O2-BISBAMP system as a function of −log [H^+] ($T_L = T_{Co}$ = 2.00 × 10^{-3} M). (b) Species distribution diagram of the 2:1 Cu(II)–O2-BISBAMP system as a function of −log [H^+] ($T_L = {}^1/_2T_{Co}$ = 2.00 × 10^{-3} M).

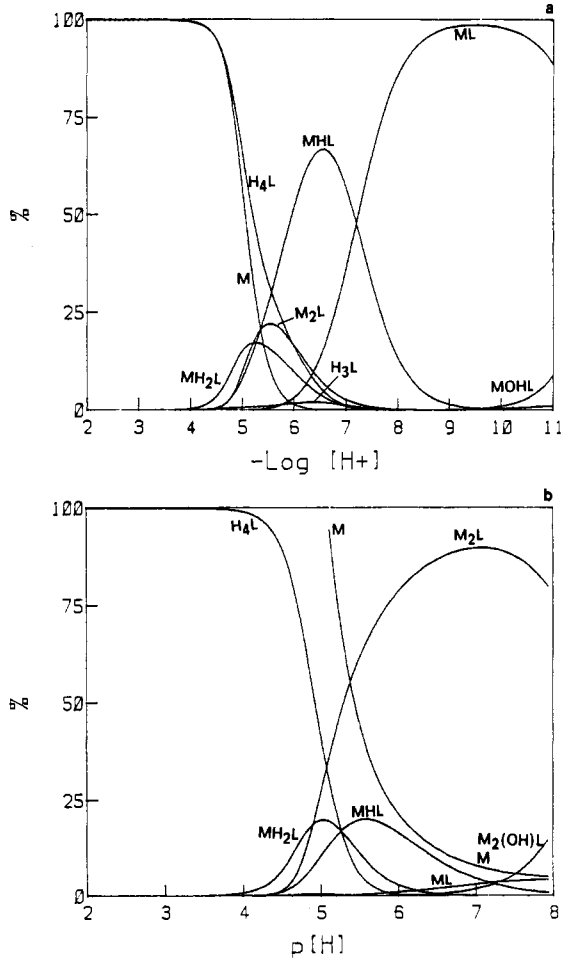

Figure 5. (a) Species distribution diagram of the 1:1 Ni(II)–O2-BISBAMP system as a function of −log [H^+] ($T_L = T_{Ni}$ = 2.00 × 10^{-3} M). (b) Species distribution diagram of the 2:1 Ni(II)–O2-BISBAMP system as a function of −log [H^+] ($T_L = {}^1/_2T_{Ni}$ = 2.00 × 10^{-3} M).

K_{ML} of the 1:1 copper(II) chelate of BAMP has been determined[15] and is available for comparison with those of the three macrocycles (Table II). BAMP binds more strongly to Cu(II) than any of the macrocycles. Thus, it appears likely that in the macrocyclic

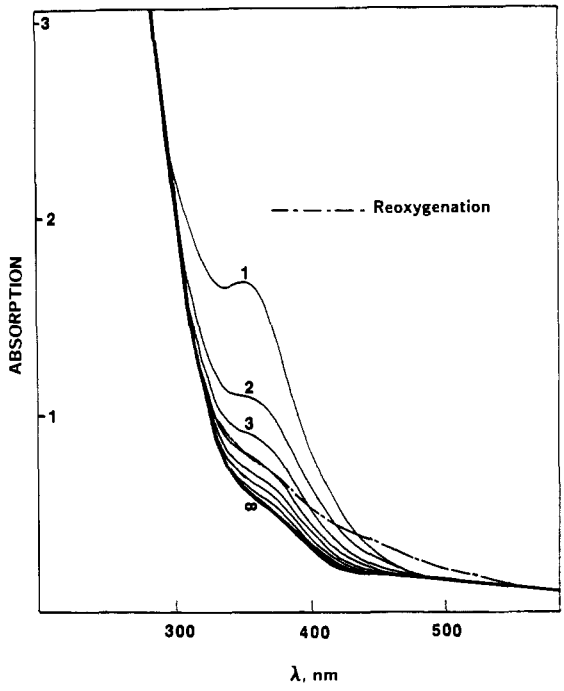

Figure 6. Absorbance of the O2-BISBAMP cobalt dioxygen complex as a function of time under an inert atmosphere (λ = 370 nm, $T_{Co} = 2T_L = 4.01 \times 10^{-4}$ M, μ = 0.100 M (KCl), p[H] = 7.45, t = 25 °C, spectra taken at 30-min intervals).

complexes Cu(II) is bound to only one of the BAMP units. The formation constants K_{ML} of the four metal ions with the macrocycle O2-BISBAMP are slightly smaller than those of the macrocycle O-BISBAMP and can be considered to be equal within experimental error.

The macrocycle C-BISBAMP forms much weaker mononuclear complexes, with binding constants about 1.6–2.2 log units lower than those of the ether-bridged macrocycles. The decrease in the K_{ML} formation constant must be attributed to the difference in the nature of the bridging chain between the two BAMP moieties. It is proposed that the C-BISBAMP macrocycle is much less preorganized, with the hydrocarbon chains collapsed together by hydrophobic binding, which must be overcome to form the coordination sphere cavity when the ligand combines with the first metal ion. Similar behavior has previously been pointed out for mononuclear complexes of C-BISTREN.[9]

A comparison of the stability constants of the K_{M_2L} type dinuclear complexes of O2-BISBAMP with those of O-BISBAMP shows that the mononuclear complex of the macrocycle with the longer bridge forms more stable binuclear complexes for all metal ions studied except Zn(II). The crystal structures of four binuclear complexes of the Schiff base analogues of O2-BISBAMP (R′ = CH_3, **5**) have been reported for M = Pb(II)[16] and M = Cu(II).[17] It is suggested that the greater separation between metal centers in O2-BISBAMP compared to that in O-BISBAMP decreases the Coulombic repulsion that is felt by the second added metal ion. The distribution of species in the 2:1 systems (Figures 3b, 4b, and 5b) in the case of Co(II) and Ni(II) shows clearly that the binuclear complexes start to form at p[H] = 5 and become the predominant species at p[H] = 7, whereas the concentration of $M_2L(OH)$ never exceeds 25%. This illustrates the low tendency of O2-BISBAMP to form hydroxy-bridged binuclear complexes with these metal ions. This behavior is very different from that of O-BISBAMP. Indeed, in the case of 2:1 solutions, binuclear complexes of O-BISBAMP begin to form at p[H] = 5, but whereas the concentration of $M_2L(OH)$ increases continuously as the p[H] is raised, M_2L is only a minor species in solution, illustrating again the strong tendency of O-BISBAMP to form the hydroxy-bridged binuclear complex. This behavior is further supported by the fact that the dioxygen adduct of the binuclear Co^{II}_2(O2-BISBAMP) complex is weaker than that of the corresponding adduct from Co^{II}_2(O-BISBAMP) and does not result in a strongly bound peroxo moiety, which would have stabilized the binuclear complex. On the other hand, the binuclear copper(II) complex of O2-BISBAMP hydrolyzes to form stable $M_2L(OH)_n$ species (n = 1, 2, 3). The high stability of $M_2L(OH)$ indicated by the relatively low pK for the addition of the first hydroxide to M_2L is strong evidence of the formation in solution of a bridging hydroxide ion. The crystal structures of three different bridged binuclear complexes $Cu^{II}_2L'(\mu\text{-}X)$ (X = N_3^-, imidazolato, OH^-), where L′ is the Schiff base analogue of O2-BISBAMP (**5**) have been reported,[16] and the complexes have been shown to display antiferromagnetic coupling of the two Cu(II) ions.

Such a contrast in the behavior of Cu(II) compared to that of the other metal ions was also shown for C-BISBAMP. Although binuclear complexes of Co(II), Ni(II), and Zn(II) do not form with C-BISBAMP, evidence for the formation of binuclear Cu(II) complexes was confirmed by a solution study[1] and a crystal structure determination.[1,18] No evidence for a bridging hydroxide was found either in solution or in the solid state. However, the binucleating tendency of three-atom-, four-atom-, and five-atom-bridged Schiff base analogues of C-BISBAMP (**7**–**9**) have been well established by Nelson et al.[19,21,22] both in nonaqueous solvents and in the solid state. For the small macrocycle **7**,[19] a dicopper(II) complex was structurally characterized in which the two Cu(II) atoms are linked by single hydroxo and single methoxo bridges, respectively. It is interesting to note that Schaber et al.[20] have reported the structure of a tetrabromide of the (1,5,9,13,17,21-hexaazacyclotetracosane)dicopper(II) complex crystallized from water that did not contain a bridge between the two copper ions. Recently the structure of a dimanganese(II) complex with a 1,1-N-bridged thiocyanate and a bridging methoxide group has been published for the macrocycle **8**.[21] A dilead(II) complex of the macrocycle **9**[22] was prepared, and its crystal structure revealed the presence of a 1,1-thiocyanate-*N* group bridging the two metal centers.

Cu(II) is known to have a high affinity for polyamine ligands; thus, binuclear complexes of Cu(II) and polyamine macrocyclic ligands have been found in many of these studies. However, the tendency toward formation of a bridge seems to depend less on the nature of the metal in M_2L complexes and more on the ability of the macrocycle to provide the proper spacing between the two metal ions. From this comparison of the three macrocycles **2**, **3**, and **4**, it is concluded that O-BISBAMP has the most favorable spacing between the two coordinating subunits for the inclusion of a bridging substrate about the size of the hydroxide ion.

As has been previously stated in this section about the coordination number of M(II) in 1:1 ML complexes, the data obtained do not support a structure in which the metal ion is coordinated to both BAMP units. However, McCann et al.[23] have determined the crystal structure of the mononuclear Co(II) and Fe(II) complexes of the Schiff base analogue of O2-BISBAMP (**5**) and have found that both these metal chelates exhibit a coordination number of 6 by binding to all six nitrogen atoms. In order to investigate the probable coordination of the mononuclear species in solution, the binding constants of M to H_iL (i = 0, 1, 2) were calculated from the data in Tables II and III. If one assumes the completion

(15) Martell, A. E.; Smith, R. M. *Critical Stability Constants*; Plenum: New York, 1982; Vol. 5.
(16) Rodgers, A.; McCann, M.; Nelson, M.; Drew, M. G. B. *J. Chem. Soc., Chem. Commun.* **1978**, 415.
(17) Drew, M. G. B.; McCann, M.; Nelson, M. *J. Chem. Soc., Chem. Commun.* **1979**, 481; **1981**, 1868.
(18) Comarmond, J. These Docteur-Ingenieur, Strasbourg, France, 1981.
(19) Drew, M. G. B.; Esho, F.; McKee, V.; Nelson, M. *J. Chem. Soc., Dalton Trans.* **1982**, 1837.
(20) Schaber, P. M.; Fettinger, J. C.; Churchill, M. R.; Nelewajek, D.; Fries, K. *Inorg. Chem.* **1988**, *27*, 1641.
(21) Raghunathan, S.; Stevenson, C.; Nelson, J.; McKee, V. *J. Chem. Soc., Chem. Commun.* **1989**, 5.
(22) Murphy, B. P.; Nelson, J.; Nelson, M.; Drew, M. G. B.; Yates, P. C. *J. Chem. Soc., Dalton Trans.* **1987**, 123.
(23) McCann, M.; Nelson, M.; Dew, M. G. B. *Inorg. Chim. Acta* **1980**, *41*, 213.

of a coordination number of 6 for the mononuclear complexes in solution, one should certainly see a dramatic increase in the difference between the successive binding constants of M(II) to H_2L and HL and M(II) to L. Nitrogen coordination higher than 3 is unlikely in MH_2L or MHL, where M(II) is expected to bind to one BAMP unit while the proton(s) is (are) located on the opposite binding moiety. For the macrocycle O2-BISBAMP, it is seen that the binding constants of M(II) to H_iL increase steadily by an average value of 1.8 log units as i decreases. For O-BISBAMP, there is also an increase, which is larger for the first step (MH_2L–MHL) than the second. For a change in coordination from one to two BAMP units, a much larger increase should be expected in going from MH_iL to ML. Therefore, there is strong evidence from solution studies that the structure of the mononuclear complex is solution can be represented by the metal ion bound to one and only one terdentate BAMP unit. Solvation of the ether oxygens by water molecules might prevent the two BAMP moieties from binding to the same metal, a process that would require at least partial desolvation of the ether oxygens.

Acknowledgment. R.M. acknowledges a Convention Ciffre Scholarship from the French Ministry of Research and Technology. Appreciation is expressed for financial support from the Office of Naval Research, under Grant No. N00014-88K-0451.

Registry No. **4**, 75620-07-4; **4**·4HCl, 123726-19-2; **6**, 75620-06-3; Co, 7440-48-4; Cu, 7440-50-8; Zn, 7440-66-6; Ni, 7440-02-0; Pb, 7439-92-1; 2,6-pyridinedicarboxaldehyde, 5431-44-7; 1,8-diamino-3,6-dioxaoctane, 929-59-9.

Contribution from the Laboratoire de Cristallochimie et de Chimie Structurale, UA (CNRS) 424, Institut le Bel, Université Louis Pasteur, 4, rue B. Pascal, F-67070 Strasbourg, France, and Institut für Physik, Medizinische Universität, Ratzeburger Allee 160, D-2400 Lübeck 1, FRG

Synthesis, Structure, and Spectroscopic Properties of Five-Coordinate Mercaptoiron(II) Porphyrins. Models for the Reduced State of Cytochrome P450

M. Schappacher,[1] L. Ricard,[1] J. Fischer,[1] R. Weiss,*[,1] R. Montiel-Montoya,[2] E. Bill,[2] and A. X. Trautwein*[,2]

Received November 29, 1988

The five-coordinate, high-spin (S = 2) (ethanethiolato)- and (tetrafluorobenzenethiolato)iron(II) "picket-fence" porphyrin derivatives [Fe($TP_{piv}P$)(SC_2H_5)][Na(C222)] (**1**), [Fe($TP_{piv}P$)(SC_6HF_4)][Na(C222)] (**2**), and [Fe($TP_{piv}P$)(SC_6HF_4)][Na(C18c6)] (**3**) have been synthesized and characterized. The X-ray structure of the chlorobenzene solvate of **1** has been determined. [Fe($TP_{piv}P$)(SC_2H_5)][Na(C222)]·C_6H_5Cl ($C_{90}H_{110}N_{10}O_{10}$ NaSClFe) crystallizes in the monoclinic system with a = 23.394 (7) Å, b = 21.762 (7) Å, c = 17.890 (6) Å, β = 103.62 (2)°, Z = 4, and space group $P2_1/n$ (Cu Kα radiation). The average Fe–N_p bond distance is 2.074 (10) Å. The displacement of iron out of the 4 Np mean plane is 0.44 Å. The ethanethiolato axial ligand of iron lies in the molecular cavity formed by the four pivalamido groups of the picket-fence porphyrin. The Fe–S bond distance of 2.324 (2) Å is in complete agreement with the Fe–S bond length found in the reduced ferrous state of cytochrome P450 by EXAFS spectroscopy. Experimental Mössbauer spectra of **1**–**3** exhibit isomer shifts that are typical for five-coordinate ferrous high-spin porphyrins and that are practically identical with that reported for reduced P450. Additionally the observed quadrupole splitting (ΔE_Q) of **1**–**3** is comparable to that of reduced P450, and especially the temperature dependence of ΔE_Q from **3** between 4.2 and 200 K is very similar to that of the reduced enzyme. The Mössbauer spectra measured under an applied field (6.4 T $\perp$ γ) in the temperature range 1.8–200 K were analyzed by the usual spin Hamiltonian formalism. The resulting zero-field splitting and hyperfine structure derived for **1** and **3**, respectively, are very close to what was found for reduced P450. Comparing the spectroscopic properties of five-coordinate mercaptoiron(II) porphyrins with those reported for the reduced state of cytochrome P450, we conclude that the cysteinate ligand remains bonded to iron in the ferrous state and is not protonated when reduction of the ferric to the ferrous state of P450 takes place.

Introduction

Both mammalian and bacterial cytochromes P450 show a common reaction cycle with four well-characterized isolable states.[3] The low-spin six-coordinate ferric resting state is converted to a high-spin five-coordinate state upon substrate binding. Reduction leads to the reduced ferrous state, in which iron is also five-coordinate. This form is converted to the oxy state by O_2 uptake. High-spin ferrous P450 is thus formed by electron transfer to the high-spin ferric enzyme substrate complex state.

Although the normal reaction cycle of chloroperoxidase (CPO) dose not involve the intermediacy of a ferrous derivative, such a state can be produced by anaerobic reduction of the high-spin ferric state of this enzyme.[3]

The spectroscopic properties of the reduced ferrous state of P450 and the reduced ferrous form of CPO have been extensively explored and have consistently been found to be quite similar to each other as well as to the properties of five-coordinate high-spin ferrous porphyrin thiolate model complexes.[4-15] The recent publications of the crystal structures of high-spin ferric $P450_{CAM}$[16] and that of the resting state of $P450_{CAM}$[17] have confirmed directly that a cysteinate ligand is bonded to iron in these two states of $P450_{CAM}$. EXAFS spectroscopy has been used to examine ferrous $P450_{CAM}$.[15] The EXAFS data together with the crystallographic results,[8] which we published several years ago for the thiolate model complex [Fe(TPP)(SEt)]$^-$, strongly suggested that the

(1) Université Louis Pasteur.
(2) Medizinische Universität.
(3) Dawson, J. H.; Sono, M. *Chem. Rev.* **1987**, *87*, 1255 and references therein.
(4) Keller, R. M.; Wüthrich, K.; Debrunner, P. G. *Proc. Natl. Acad. Sci. U.S.A.* **1972**, *69*, 2073.
(5) Champion, P. M.; Münck, E.; Debrunner, P. G.; Moss, T. H.; Lipscomb, J. D.; Gunsalus, I. C. *Biochim. Biophys. Acta* **1975**, *376*, 579.
(6) Chang, C. K.; Dolphin, D. *J. Am. Chem. Soc.* **1975**, *97*, 5948.
(7) Chang, C. K.; Dolphin, D. *Proc. Natl. Acad. Sci. U.S.A.* **1976**, *73*, 3338.
(8) Caron, C.; Mitschler, A.; Rivière, G.; Ricard, L.; Schappacher, M.; Weiss, R. *J. Am. Chem. Soc.* **1979**, *101*, 7401.
(9) Parmely, R. C.; Goff, H. M. *J. Inorg. Biochem.* **1980**, *12*, 269.
(10) Budyka, M. F.; Khenkin, A. M.; Shteinman, A. A. *Biochem. Biophys. Res. Commun.* **1981**, *101*, 615.
(11) Okubo, S.; Nozawa, T.; Hatano, M. *Chem. Lett.* **1981**, 1625.
(12) Battersby, A. R.; Howson, W.; Hamilton, A. D. *J. Chem. Soc., Chem. Commun.* **1982**, 1266.
(13) Schappacher, M.; Ricard, L.; Weiss, R.; Montiel-Montoya, R.; Gonser, U.; Bill, E.; Trautwein, A. X. *Inorg. Chim. Acta* **1983**, *78*, L9.
(14) Cramer, S. P.; Dawson, J. H.; Hodgson, K. O.; Hager, L. P. *J. Am. Chem. Soc.* **1978**, *100*, 7282.
(15) Hahn, J. E.; Hodgson, K. O.; Anderson, L. A.; Dawson, J. H. *J. Biol. Chem.* **1982**, *257*, 10934.
(16) Poulos, T. M.; Finzel, B. C.; Gunsalus, I. C.; Wagner, G. C.; Kraut, J. *J. Biol. Chem.* **1985**, *260*, 16122.
(17) Poulos, T. L.; Finzel, B. C.; Howard, A. J. *Biochemistry* **1986**, *25*, 5314.

0020-1669/89/1328-4639$01.50/0